The DEAD Box Protein eIF4A. 2. A Cycle of Nucleotide and RNA-Dependent Conformational Changes†

Jon R. Lorsch and Daniel Herschlag*

Department of Biochemistry, Beckman Center, B400, Stanford University, Stanford, California 94305-5307

Received October 1, 1997; Revised Manuscript Received December 23, 1997

ABSTRACT: Limited proteolysis experiments have been carried out with the DEAD box protein eIF4A. The results suggest that there is a substantial conformational change in eIF4A upon binding single-stranded RNA. Binding of ADP induces conformational changes in the free enzyme and the enzyme•RNA complex, and binding of the ATP analogue AMP−PNP induces a conformational change in the enzyme•RNA complex. The presence or absence of the γ-phosphate on the bound nucleotide acts as a switch, presumably via the Walker motifs, that mediates changes in protein conformation and, as described in the preceding paper in this issue, also mediates changes in RNA affinity. Thus, these results suggest that there is a series of changes in conformation and substrate affinity throughout the ATP hydrolysis reaction cycle. A model is proposed in which eIF4A and the eIF4A-like domains of the DEAD box proteins act as ATP-driven conformational switches or motors that produce movements or structural rearrangements of attached protein domains or associated proteins. These movements could then be used to rearrange RNA structures or RNA•protein complexes.

eIF4A is an RNA-activated ATPase (*1, 2*) that facilitates binding of the 40S ribosomal subunit to eukaryotic mRNAs (*3, 4*). It is the archetypal member of the DEAD box family of proteins, as the other members of this family are made up of core eIF4A-like domains flanked by N- and C-terminal extensions (*5*). eIF4A can unwind small duplex RNAs in vitro in conjunction with another factor, eIF4B (*2, 6*−*9*). These and other observations have led to the proposal that the DEAD box proteins function as RNA helicases (*2, 6, 8, 10*−*13*). Nevertheless, few details of the molecular functions or mechanisms of these enzymes are known.

In the preceding paper in this issue, a minimal kinetic and thermodynamic framework for the eIF4A-catalyzed ATP hydrolysis reaction was established (*14*). It was demonstrated that the enzyme's affinity for RNA is modulated by the presence or absence of the γ-phosphate on the bound nucleotide. In addition, UV-induced RNA cross-linking experiments suggested that the presence or absence of the γ-phosphate also alters the conformation of the enzyme (*9, 14*).

To further explore ligand-induced conformational changes in eIF4A, limited proteolysis experiments were performed. These experiments provide evidence that distinct conformations of the enzyme are stabilized upon binding of the various combinations of substrates and products. The γ-phosphate of the bound nucleotide plays a key role in inducing both the conformational changes and changes in RNA affinity, suggesting that ATP binding and hydrolysis produce a cycle of conformational and RNA affinity changes in eIF4A. It is proposed that eIF4A and the eIF4A-like domains of the other DEAD box proteins act as ATP-dependent motors that produce motions in attached protein domains or associated proteins. Motions in these domains or associated proteins could then induce structural rearrangements in RNAs or RNA−protein complexes.

EXPERIMENTAL PROCEDURES

Materials. SP6 RNA polymerase was from United States Biochemicals; ultrapure ATP and poly(U) were purchased from Pharmacia; AMP−PNP,[1] ADP, chymotrypsin, subtilisin, 5-bromouridine triphosphate, and L-BAPNA were from Sigma; ATP-γS was from Boehringer Mannheim; tosyl-L-phenylalanine chloromethyl ketone-treated trypsin was from Worthington; immobilon-P membrane was from Millipore; recombinant mouse eIF4AI was expressed and purified as described in the preceding paper in this issue (*14*).

RNA Concentrations. RNA concentrations and thermodynamic constants involving RNA are given in 20-mer units (nucleotide concentration divided by 20), unless otherwise noted. A 20-mer is approximately the minimal site size for RNA binding to eIF4A ((*14*−*16*); Unpublished Results).

Limited Proteolysis. Reaction buffers contained 2.5 mM $MgCl_2$, 1 mM DTT, 1% glycerol, and either 20 mM Tris−

† This work was supported by a David and Lucile Packard Foundation Fellowship in Science and Engineering to D.H. J.R.L. was supported by a Damon Runyon−Walter Winchell Foundation Fellowship (DRG 1345).

* Address correspondence to this author. Phone: 650-723-9442. Fax: 650-723-6783. E-mail: herschla@cmgm.stanford.edu.

[1] Abbreviations: ss, single-stranded; ds, double-stranded; ATP-γS, adenosine-5′-*O*-(3-thiotriphosphate); AMP−PNP, adenylylimidodiphosphate; Tris, tris(hydroxymethyl)aminomethane; MES, 2-(*N*-morpholino)ethanesulfonic acid; DTT, dithiothreitol; SDS, sodium dodecyl sulfate; P_i, inorganic phosphate; PAGE, poly(acrylamide) gel electrophoresis; L-BAPNA, *N*-(α-benzoyl)-L-arginine *p*-nitroanilide; $t_{1/2}$, half time.

S0006-2960(97)02431-8 CCC: $15.00
Published on Web 02/06/1998

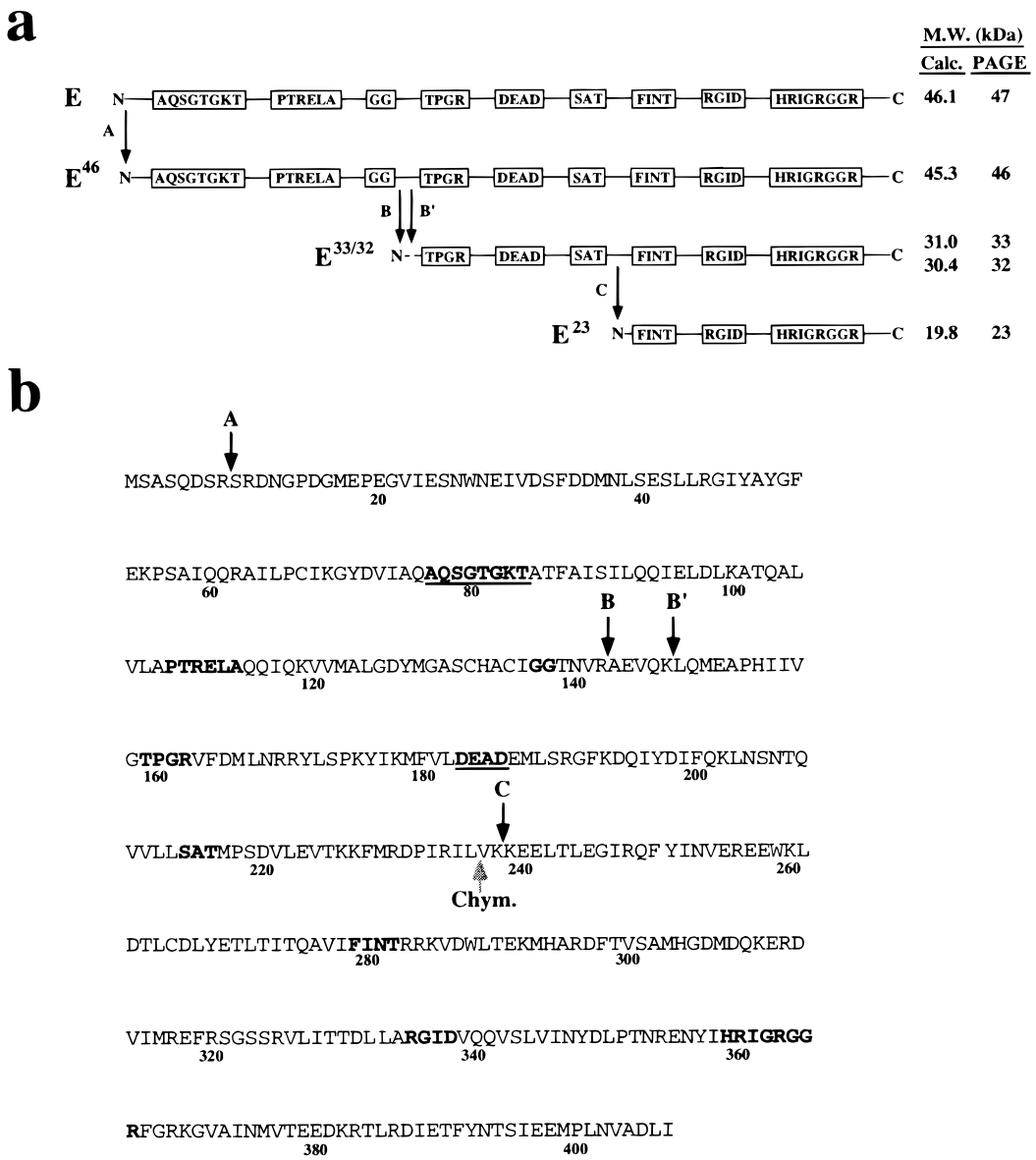

FIGURE 1: Pattern of trypsin cleavage of eIF4A. (a) The sequential trypsin cleavages, from the N- to the C-terminus, are shown by the solid arrows and are lettered A, B, B′, and C. The calculated molecular mass and molecular mass estimated from SDS−PAGE are shown on the right; the names shown on the left are based on the SDS−PAGE molecular weight estimates and are used in the text. The DEAD box consensus sequences are shown in boxes. (b) Mapping of trypsin cleavage sites. N-terminal sequencing of tryptic fragments located the cleavage sites that produced the main trypsin proteolysis fragments (black arrows). Letters in bold are highly conserved sequences in the DEAD box family of proteins (*5*), and the Walker A (AQSGTGKT) and B (DEAD) NTPase motifs are underlined. The ~23 kDa chymotryptic fragment was also sequenced (Chym., gray arrow).

Cl, pH 7.4, and 80 mM KCl or 20 mM MES−KOH, pH 6.0, and 10 mM potassium acetate. These conditions are referred to as conditions A and B, respectively, throughout. Reactions were performed under buffer conditions B at 25 °C except where noted. The concentrations of ligands used was 30 μM poly(U), 1 mM ATP·Mg^{2+}, ADP·Mg^{2+}, AMP−PNP·Mg^{2+}, or ATP-γS·Mg^{2+}, unless otherwise noted. These concentrations are sufficient to ensure the formation of the appropriate enzyme·ligand complexes with the full-length enzyme (*14*). Nucleotides were always added as the stoichiometric complex with $MgCl_2$. The concentration of eIF4A was 4 μM, and 4, 40, or 400 nM trypsin or chymotrypsin was used. The reactions were initiated by the addition of protease. Aliquots (10 μL) were removed at various times, quenched in 2% SDS, 0.1% bromophenol blue, 10% glycerol, 50 mM Tris−Cl, pH 6.8, 100 mM DTT, plus 100 mM NaOH, and then immediately boiled for 10 min. The NaOH was included to degrade the RNA; high concentrations of RNA were found to interfere with the staining of the gel. The samples were then neutralized by addition of 1 N HCl. Samples were analyzed by SDS−PAGE (*17*) on 10, 15, or 20% poly(acrylamide) gels (12 × 15 cm). Gels were stained with coomassie blue.

Half times for digestion were estimated from coomassie staining of the gels. While these estimates are crude, the results were reproducible in independent experiments and differences as small as 2-fold were readily detected, as demonstrated by serial dilution standards (not shown; see also Figure 5). However, in all cases in which 2-fold effects provided evidence of a conformational change, additional evidence to support the conclusion was also obtained.

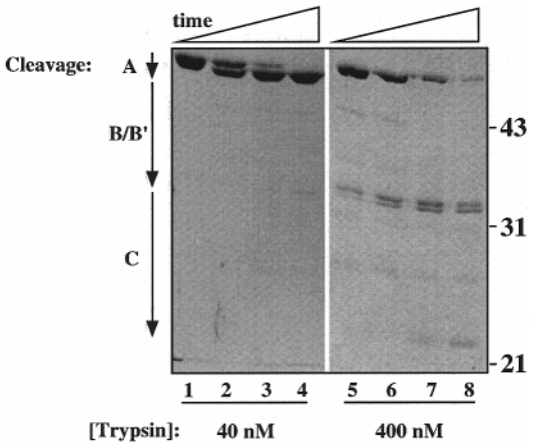

FIGURE 2: SDS−PAGE analysis showing the pattern of trypsin hydrolysis of eIF4A. eIF4A (4 μM) was digested with the indicated concentrations of trypsin in the absence of ligand. The cleavages referred to as A, B/B′, and C are defined in Figure 1a and are shown schematically by arrows on the left. The positions of molecular mass markers are shown on the right (kDa).

The possibility that the changes in protease sensitivities observed for the various enzyme−substrate complexes result from changes in protease activity rather than changes in the conformation of eIF4A was tested as follows. The activity of trypsin was measured using the chromogenic substrate L-BAPNA in the presence and absence of the ligands used in the limited proteolysis experiments (see "Trypsin Activity Assays" below). There were no large effects on trypsin activity, the largest being a 1.8-fold decrease in the initial rate of L-BAPNA hydrolysis upon addition of poly(U) (30 μM; data not shown). Thus, the increases in the rates of proteolysis in the presence of poly(U) described in the Results section may slightly *underestimate* the true values, but no conclusions are affected. Neither AMP−PNP·Mg^{2+} nor ADP·Mg^{2+} (1 mM) had any effect on trypsin activity. The combination of 1 mM AMP−PNP·Mg^{2+} or ADP·Mg^{2+} plus 30 μM poly(U) had the same small inhibitory effect as poly(U) alone.

Increased protease sensitivity of the E·ssRNA complex relative to the free enzyme could be caused by neutralization of the positive charge on eIF4A that would otherwise inhibit binding of trypsin or by poly(U) binding to trypsin, thereby increasing the local concentration of the protease around eIF4A. However, increased protease sensitivity in the presence of poly(U) is also seen with chymotrypsin, rendering these possibilities unlikely. Furthermore, an increase in protease sensitivity is observed with ssRNAs as small as U_{20} (data not shown), which represents the approximate site size for RNA binding to eIF4A.

Additional evidence that the changes in proteolysis rates are due to changes in eIF4A and not to changes in protease activity is provided by the similarity between estimates of the $K_{1/2}$ values (the concentration of ligand at which the effect on proteolysis is half-maximal) for the ligands and their measured K_d values (*14*). With both trypsin and chymotrypsin, the estimated $K_{1/2}$'s for AMP−PNP·Mg^{2+} and ADP·Mg^{2+} are approximately the same as the measured K_d's (Figure 6b in the Results section): 50−100 μM for AMP−PNP·Mg^{2+} binding to the E·ssRNA complex vs a measured K_d of 60 μM; 10−25 μM for ADP·Mg^{2+} binding to the E·ssRNA complex vs a measured K_d of 8 μM. A value of ~3 μM for the $K_{1/2}$ of poly(U) (not shown) may reflect a titration point because of the high concentration of eIF4A (4 μM) required for these experiments. The value of 3 μM, therefore, is expected to represent a lower limit for the dissociation constant; the measured K_d is 5 μM (*14*).

Pulse−Chase Proteolysis Experiment. eIF4A (4 μM) was digested with 400 nM trypsin (200-μL volume; buffer and conditions as above). Aliquots (40 μL) were removed after 60 min ($t_2 = 0$) and added to each of the following: 0.6 μL of water; 0.3 μL of 3 mM poly(U) (22 μM final; 20mer units); 0.6 μL of 50 mM AMP−PNP·Mg^{2+} (750 μM final); or 0.6 μL of 50 mM ADP·Mg^{2+} (750 μM final). Aliquots (10 μL) of each of these reactions were removed at various times and quenched and analyzed as described above.

N-Terminal Sequence Analysis. Trypsin proteolysis reactions containing poly(U) were performed as described above and the fragments resolved by SDS−PAGE on a 10% poly(acrylamide) gel. The gel was electro-blotted onto immobilon-P membrane (*17*). The blot was stained with coomassie blue, and the bands were excised. Sequencing was performed at the W. M. Keck Foundation Biotechnology Resource Laboratory at Yale University. At least eight amino acids were positively assigned for each fragment. Proteolysis near the C-terminus of the enzyme cannot be detected by N-terminal sequencing, and thus, the possibility that several residues have also been lost from the C-terminus in any of the fragments cannot be ruled out.

Trypsin Activity Assays. Reactions were performed in buffer B at 25 °C in quartz cuvettes. The reactions contained 10 μM L-BAPNA and either no ligand or the same concentrations of poly(U), AMP−PNP·Mg^{2+}, or ADP·Mg^{2+} as were used in the limited proteolysis experiments. The reactions were started by the addition of trypsin to a final concentration of 200 nM and monitored for 100 min at 410 nm in a Uvikon UV/vis spectrophotometer (Kontron Instruments). The experiment was performed under subsaturating substrate conditions, and cleavage of the amide linkage is the rate-limiting step using this substrate (*18*). No hydrolysis of the substrate was detected after 100 min in the absence of trypsin.

Determination of Steady-State Parameters for ATP Hydrolysis by the E^{46} Fragment. eIF4A (4 μM) was incubated for 45 min in the absence of ligands either with or without 80 nM trypsin, as described above ("*Limited Proteolysis*"). The reactions were quenched by addition of the irreversible trypsin inhibitor 4-(2-aminoethyl)benzenesulfonyl fluoride (AEBSF) to 250 μM. Aliquots of the digestion and control reactions were then used in steady-state kinetic experiments. The initial rates of ATP hydrolysis (1 mM ATP·Mg^{2+}) as a function poly(U) concentration were measured as described in the preceding paper in this issue (*14*), using excess poly(U) and ATP·Mg^{2+} over enzyme and a concentration range of poly(U) from 5-fold below the K_m to 10-fold above it. K_m for poly(U) and k_{cat} (assuming that 1 mM ATP·Mg^{2+} is saturating for E^{46}, as it is for the full-length enzyme) were determined from these data as described previously (*14*). Samples were analyzed by SDS−PAGE to ensure that >95% of the digested protein was in the form of the E^{46} fragment and that no further proteolysis took place during the ATPase assays (data not shown). The observed reactions cannot be accounted for by the small amount of undigested eIF4A remaining.

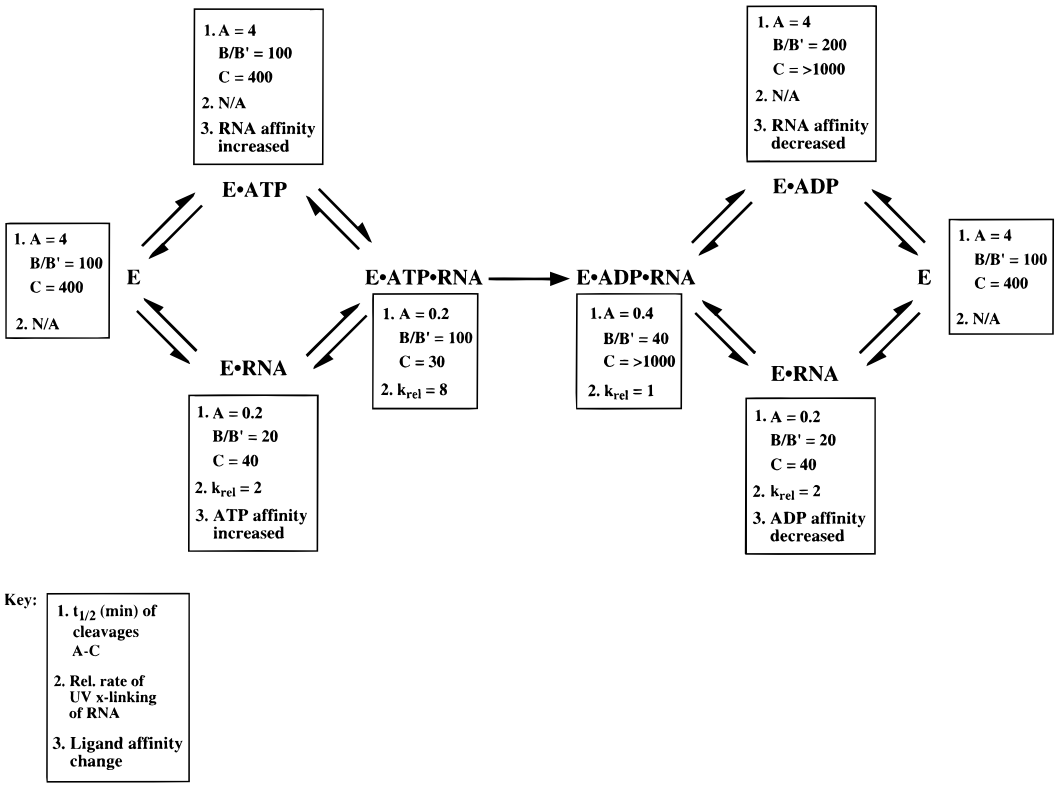

FIGURE 3: Summary of the evidence for conformational changes in eIF4A upon ligand binding. The mechanistic scheme for the RNA-dependent ATP hydrolysis reaction is shown (*14*). The boxes above each enzyme species indicate the properties of that species: (1) Half times (min) for cleavages A, B/B′, and C (see Figure 1a and Table 1); (2) relative rate of UV cross-linking of RNA to each species (rates are relative to that for the E·RNA·ADP complex (*14*)); (3) the change in ligand affinity for each state (*14*). For the proteolysis data (1 above), AMP−PNP was used in place of ATP; as described in the Results section, the proteolysis effects of ATP and AMP−PNP are similar, but hydrolysis complicates the analyses with ATP (see "ATP Binding and Conformational Changes"). N/A, not applicable.

RESULTS

Limited proteolysis experiments were performed in order to characterize the ligand-dependent conformational changes of eIF4A. The basis of these experiments is that different conformational states of a protein may have different regions more or less exposed and thus more or less susceptible to cleavage by a protease. The results from these experiments with eIF4A are described in the following sections after first outlining the positions and relative rates of the proteolytic cleavage events.

Pattern of Proteolytic Cleavage of eIF4A

The pattern of eIF4A cleavage produced by trypsin is summarized in Table 1 and Figure 1. Hereafter, the fragments are named for their apparent molecular weights on SDS−PAGE: E^{46}, referring to the 46 kDa fragment, etc. (Table 1 and Figure 1a). There is a sequential pattern of appearance of proteolysis products, as depicted schematically in Figure 1a, resulting from the different rate constants for the individual cleavages. The relative rates of the cleavages can be seen in Figure 2, in which the product from cleavage A (lanes 1−3) is observed earlier than the products from cleavages B and B′ (lanes 4−7). The products from cleavages B/B′ are, in turn, observed earlier than the product from cleavage C (lanes 7 and 8; a higher trypsin concentration is used in lanes 5−8 to decrease the time required for formation of the later products). The rate constants for each cleavage can vary upon ligand binding to the enzyme, as described in detail below.

The positions of the cleavages were mapped by N-terminal sequencing of the fragments and are summarized in Figure 1b. As expected, all of the trypsin cleavage sites occur after lysine or arginine residues. Each cleavage occurs between, rather than within, highly conserved DEAD box sequence motifs (Figure 1b). The regions in which the cleavages occur are nonconserved, varying in length, and sequence from one DEAD box protein to another (*5*). This suggests that these regions may include surface regions of the enzyme. Such regions are expected to be more conformationally mobile and more accessible to proteolysis than core regions of the protein. Indeed, in the crystal structure of the Rep DNA helicase, which shares sequence homology with eIF4A (*19, 20*), the regions of Rep expected to correspond to cleavage positions B/B′ and C are surface loops (*21*).

With chymotrypsin, fragments of 46.5, 41, 33, 24, and 23 kDa are produced (Figure 4b). These fragments are of similar size to those produced by trypsin proteolysis, suggesting that certain regions of eIF4A are accessible and can be cleaved by trypsin or chymotrypsin. The position of the cleavage that generates the 23 kDa fragment was mapped to Leu236, only two residues away from trypsin cleavage site C (Figure 1b); the other cleavage positions were not determined.

Conformational Changes in eIF4A

The proteolysis data outlined below, coupled with the changes in UV cross-linking of RNA to eIF4A and the

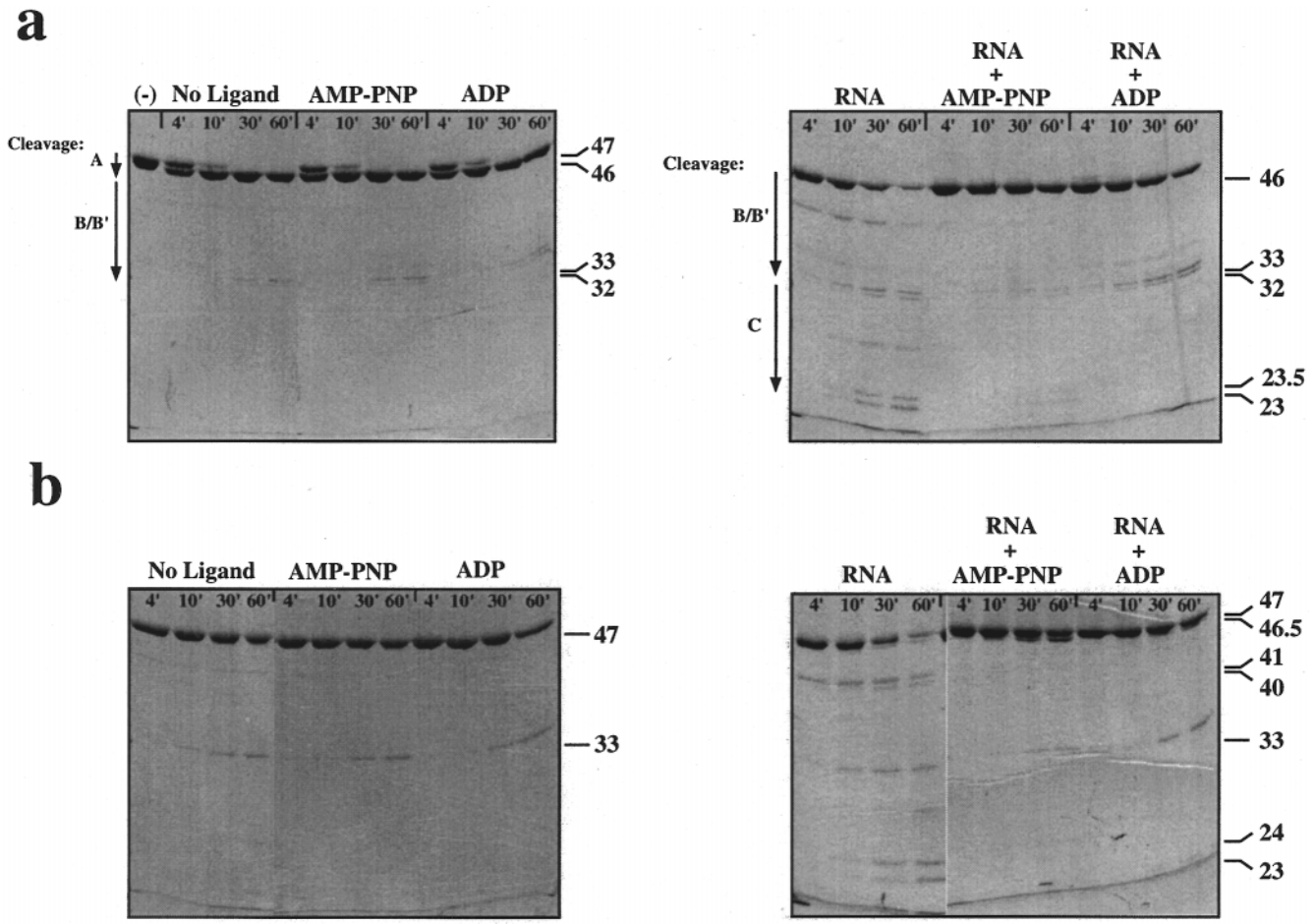

FIGURE 4: Analysis of trypsin (a) and chymotrypsin (b) cleavage. SDS−PAGE analysis of time courses of cleavage of eIF4A (4 μM) by 40 nM trypsin (a) or chymotrypsin (b) in the absence of ligands or presence of saturating concentrations of AMP−PNP, ADP, or poly(U) (RNA). In panel a, each cleavage is denoted schematically on the left by an arrow. In the right-hand panel of a, cleavage A is already complete by the 4′ time point so that the predominant band is E^{46}. The approximate size of each fragment (kDa) is indicated on the right. (−) No protease.

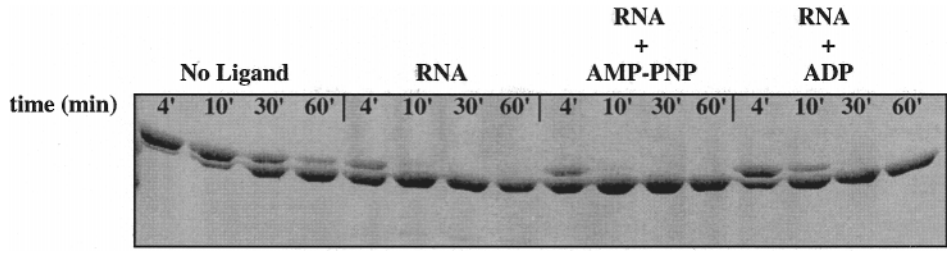

FIGURE 5: Ligand binding affects the rate of trypsin cleavage at site A. A low concentration of trypsin (4 nM) was used to follow the first cleavage of eIF4A (cleavage A, Figure 1a). SDS−PAGE analysis of time courses in the absence of ligand or presence of saturating concentrations of ssRNA [poly(U)], AMP−PNP, or ADP.

nucleotide-dependent changes in ssRNA affinity described in the preceding paper in this issue, suggest that eIF4A undergoes ssRNA- and nucleotide-dependent conformational changes.[2] The data from all of these experiments are summarized Figure 3. The proteolysis experiments are summarized in Table 1 and described in detail in the following sections.

Binding of ssRNA Results in a Change in eIF4A Conformation. Addition of ssRNA produces a large increase in the susceptibility of eIF4A to proteolysis. In the absence of ligand, eIF4A is cleaved by trypsin with a half time ($t_{1/2}$) of ~4 min to produce E^{46} (Figure 4a, RNA lanes, and Table 1). However, with saturating poly(U), cleavage A (Figure 1a) was complete by 4 min (Figure 4a). Lower concentrations of trypsin were therefore used to estimate the effect of poly(U) on the rate of cleavage A. The time courses shown in Figure 5, obtained using 10-fold less trypsin than in Figure 4a, show that poly(U) accelerates the cleavage ~20-fold (e.g., compare No Ligand 60-min lane and RNA 4-min lane in Figure 5). The half time for cleavage with saturating poly(U) and 4 nM trypsin of ~2 min corresponds to a half time

[2] In general, conformational changes identified in proteolysis, cross-linking, and related experiments can reflect changes in the ground state of an enzyme·ligand complex or in a higher energy state. Lowering the energy of a high-energy state could increase its population sufficiently to allow detection by proteolysis or cross-linking. Each of these possibilities represent potentially functionally relevant conformational changes, and no distinction is made between them in the text.

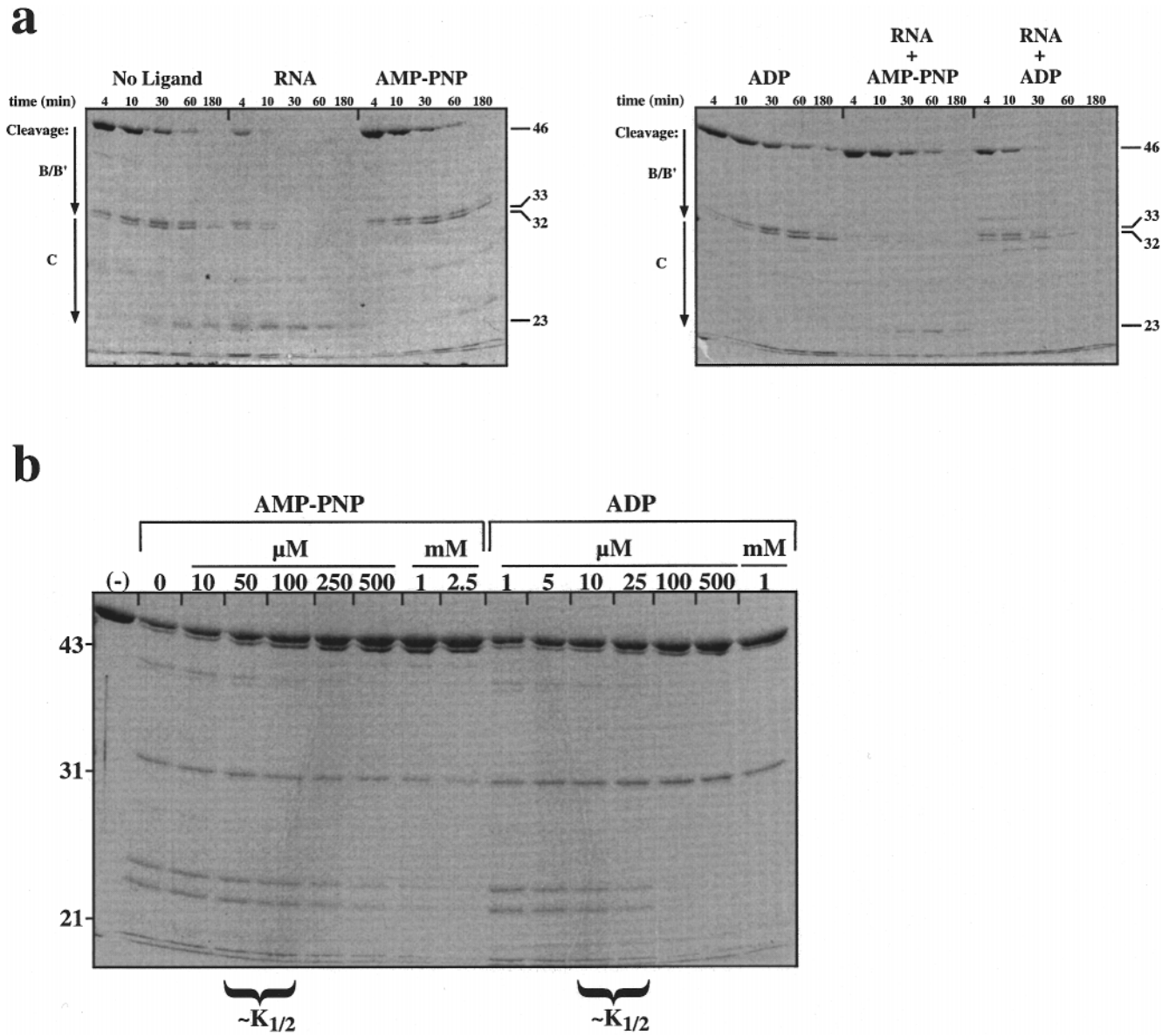

FIGURE 6: More extensive proteolysis of eIF4A allows detection of additional conformational states. (a) SDS−PAGE analysis of time courses for trypsin (400 nM) cleavage of eIF4A (4 μM) in the absence of ligands or presence of saturating concentrations of AMP−PNP, ADP, or poly(U) (RNA). The approximate size of each fragment (kDa) is shown on the right. Each cleavage is denoted schematically on the left by an arrow; cleavage A is complete by the first time point and is therefore not depicted. The slowest migrating band is E^{46}. (b) Determination of $K_{1/2}$'s for AMP−PNP·Mg^{2+} and ADP·Mg^{2+}. The $K_{1/2}$ values are the concentrations of ligands that give the half-maximal effect on proteolysis and are expected to reflect dissociation constants. eIF4A (4 μM) was digested for 1 h with 40 nM chymotrypsin in the presence of varying concentrations of AMP−PNP or ADP. The approximate $K_{1/2}$'s were determined by visual inspection; brackets at the bottom indicate these concentration ranges. Molecular mass markers (kDa) are shown to the left of the gel. (−) lane: no protease. A similar result was obtained using trypsin and monitoring sensitivity of the 46 kDa fragment to further proteolysis (not shown).

of 0.2 min normalized to 40 nM trypsin,[3] again 20-fold faster than that obtained in the absence of poly(U) (Table 1 and Figure 4a). This accelerated cleavage suggests that binding of ssRNA stabilizes an alternate conformation of eIF4A in which this cleavage site is more exposed. Several controls described in the Experimental Procedures section strongly suggest that the increased cleavage does not arise from effects of poly(U) on trypsin's intrinsic activity.

Further support for the conclusion that poly(U) binding induces a conformational change in eIF4A is provided by the increase in the overall cleavage rate by chymotrypsin in the presence of poly(U) (Figure 4b, No Ligand vs RNA lanes, ~5-fold increase). In addition, with trypsin, a band at ~43 kDa (E^{43}) accumulates significantly only in the presence of ssRNA (Figure 4a RNA lanes vs Figures 4a and 6 No Ligand lanes; Figure 6 uses a 10-fold higher concentration of trypsin, allowing comparison of similar extents of digestion). Analysis of the cleavage patterns and rates suggests that this accumulation arises because of faster formation of E^{43} from E^{46} with bound ssRNA and not because of slower degradation

[3] Half-lives for proteolytic cleavages were assumed to change linearly with trypsin concentration over the ranges used in this study (4−400 nM) and are reported as half times at 40 nM trypsin for comparison. Support for this assumption comes from several experiments in which the half time for the same cleavage was measured at two different trypsin concentrations. For example, the half time for the A cleavage in the absence of ligand is ~4 min at 40 nM trypsin and ~20 min at 4 nM trypsin (compare "No Ligand" lanes in Figures 4a and 5).

Table 1: Estimated Half-Lives for Cleavage of the Full-Length Enzyme and Subsequent Fragments in the Presence of 40 nM Trypsin under Buffer Conditions B (Time in min); a Schematic of the Cleavage Pattern Is Shown on the Left

	no ligand	RNA	AMP−PNP·Mg^{2+}	ADP·Mg^{2+}	RNA + AMP−PNP·Mg^{2+}	RNA + ADP·Mg^{2+}
eIF-4A						
A↓	4	0.2	4	4	0.2	0.4
E^{46}						
B/B′↓	100	20	100	200	100	40
$E^{33/32}$						
C↓	400	40	400	>1000	30	>1000
$E^{23/22}$						
↓	300	600	300	not formed	600	not formed
smaller fragments[a]						

[a] The estimated $t_{1/2}$ values for degradation of $E^{22/23}$ (except "not formed") are less accurate than for cleavages A−C because $E^{23/22}$ is being created continuously during the experiment. Thus, differences are not significant. "Not formed" indicates the $E^{23/22}$ species is not formed under these conditions.

of E^{43}. This is because the rate of formation of E^{43} in the presence of ssRNA is faster than the total rate of cleavage of precursors in the absence of ssRNA. A band similar in size to E^{43} builds up in the presence of ssRNA but not the absence of ligand during chymotrypsin digestion of eIF4A (Figure 4b, compare No Ligand 60 min to RNA 10 min).

Subsequent cleavages of E^{46} also provide evidence for a conformational change upon binding of ssRNA. Under the proteolysis conditions of Figure 4a, E^{46} is stable for >60 min in the absence of ligand (No Ligand lanes). However, it is rapidly cleaved to smaller fragments in the presence of poly(U) (Figure 4a, RNA lanes). The $t_{1/2}$ value for the disappearance of E^{46} (cleavage B/B′) is increased 5−10-fold in the presence of poly(U) relative to what is observed in the absence of ligand (e.g., Figure 4a, No Ligand 30-min lane vs RNA 4-min lane). This suggests that E^{46} also binds ssRNA and undergoes a conformational change.

Although these data suggested that there is an ssRNA-dependent conformational change in E^{46}, its relevance to the behavior of full-length eIF4A was not immediately clear. The ability of the E^{46} fragment to catalyze RNA-dependent ATP hydrolysis was therefore tested. Steady-state kinetic experiments showed that E^{46} is still an ssRNA-activated ATPase. Further, it has the same K_m for poly(U) and k_{cat} as the full-length enzyme, within error (K_m of 1.8 μM vs 1.0 μM for E^{46} and the full-length enzyme, respectively; k_{cat} of 0.8 min^{-1} vs 1.0 min^{-1} for E^{46} and the full-length enzyme, respectively; data not shown; K_m for ATP was not determined). These data demonstrate that the active structure of the enzyme is maintained after cleavage at Arg8 (Figure 1b) and suggest that conformational changes in E^{46} are likely to take place in the full-length enzyme as well.

The fragment $E^{33/32}$ is also substantially more sensitive to proteolysis in the presence of ssRNA than in its absence. The $t_{1/2}$ for proteolysis is 40 min in the presence of ssRNA and 400 min in its absence (Figure 6, No Ligand lanes 30−180 min vs RNA lanes 4−10 min). Because it can be difficult to discern the rate of a cleavage event when a fragment is simultaneously being formed from larger fragments and degraded to smaller ones, a pulse−chase proteolysis experiment was performed to test whether $E^{33/32}$ is indeed more sensitive to proteolysis in the presence of ssRNA (Figure 7a). In this experiment, eIF4A was partially digested in the absence of ligands to allow accumulation of $E^{33/32}$. The $E^{33/32}$ was then chased by addition of ssRNA. As seen in Figure 7b, $E^{33/32}$ disappears faster in the presence of ssRNA than in its absence, confirming that ssRNA increases the protease sensitivity of this fragment (Figure 7b, compare chase: t_2 phase, No Ligand and RNA lanes).

The increased cleavage of $E^{33/32}$ could arise because this fragment alone can bind ssRNA and undergo a conformational change or because $E^{33/32}$ remains associated with the N-terminal fragments produced from cleavage B/B′ in a functional complex that can still bind ssRNA and undergo the conformational change. Analysis of proteolysis reactions by nondenaturing PAGE gave no indication of such a complex (not shown). However, the effects of ADP on the proteolysis of the smaller fragments described below suggest that the cleavage products remain together following cleavage B/B′.

In summary, binding of ssRNA to eIF4A produces a large increase in the susceptibility of the enzyme to proteolysis, suggesting the enzyme undergoes a conformational change when it binds ssRNA. This conformational change affects at least four sites in the enzyme separated by up to 229 amino acids in the primary structure (cleavages A through C; Figure 1b). The physical nature of this conformational change is not known, but one possibility is that the highly negatively charged N-terminus (Figure 1b) occupies the RNA binding site in the absence of RNA.

Binding of Adenosine Nucleotides Also Modulates the Structure of eIF4A. In this section, evidence is presented that the free enzyme also undergoes a conformational change when it binds ADP·Mg^{2+} and that this conformational change is distinct from that produced by ssRNA binding. In the following section, evidence is presented that ADP·Mg^{2+} and ATP·Mg^{2+} each produce distinct conformational changes upon binding to the E·ssRNA complex.

The ADP-bound form of E^{46} is less sensitive to proteolysis than the free enzyme or any of the other liganded forms (Figure 6a; this is most apparent in the 60′ and 180′ lanes; summarized in Table 1). A more striking effect is that the E^{23} cleavage product does not accumulate in the presence of ADP, even after E^{46} and $E^{33/32}$ have been degraded (Figure 6a). E^{23} is generated from all enzyme forms that lack bound ADP (Figure 6a). We therefore performed a pulse−chase proteolysis experiment to determine whether the absence of E^{23} indicates that cleavage C (Figure 1a) does not occur in the presence of ADP or whether the degradation of E^{23} is stimulated by ADP. This experiment, described above

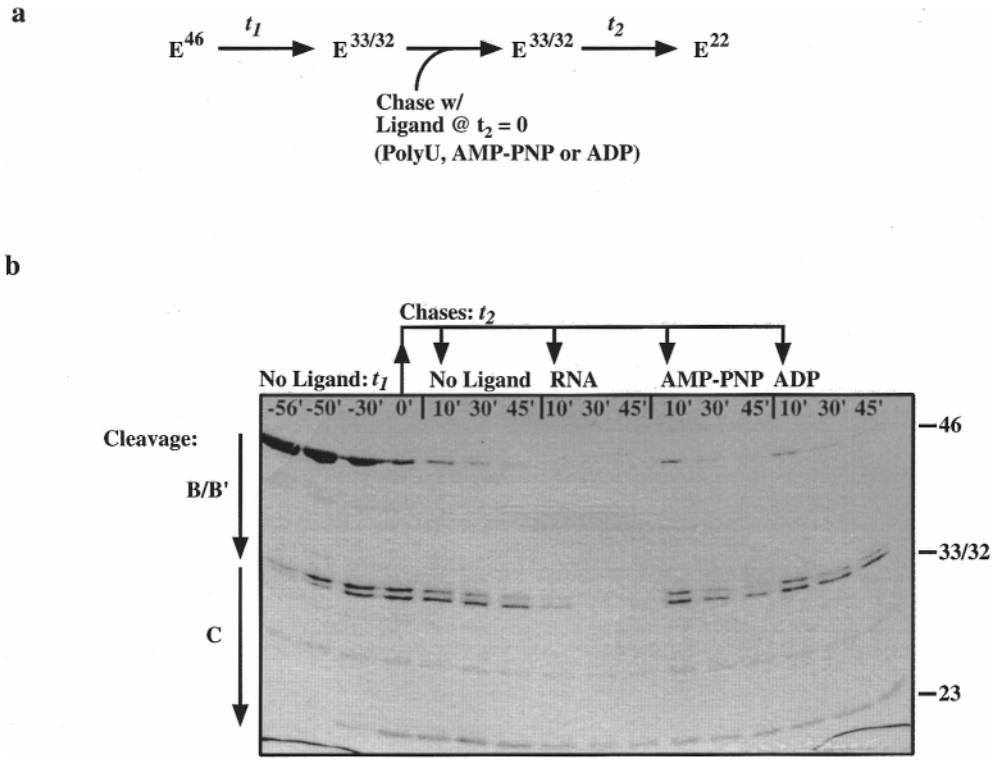

FIGURE 7: Pulse−chase experiment to probe effects of ligands on cleavage C and subsequent cleavages. (a) Schematic representation of the pulse−chase experiment. eIF4A (4 μM) was digested with 400 nM trypsin for $t_1 = 60$ min in the absence of ligand to generate the $E^{33/32}$ fragments and to deplete precursors. After formation of $E^{33/32}$, aliquots of the reaction were chased with saturating concentrations of either poly(U), AMP−PNP, or ADP. (b) Analysis of the pulse−chase experiment by SDS−PAGE. The t_1 phase began at $t = -60$ min. At $t = 0$, the t_2 phase was initiated by dividing the reaction and adding the chases with saturating ligand. A control reaction in which no ligand was added at $t_2 = 0$ was also performed (No Ligand). The cleavages are shown schematically by arrows on the left. The molecular mass (kDa) of the fragments is shown on the right. The highest molecular weight band is E^{46}.

(Figure 7a) and shown in Figure 7b, demonstrated that the degradation of E^{23} is not detectably accelerated by ADP (Figure 7b, ADP vs other lanes), indicating that absence of E^{23} accumulation in the presence of ADP arises from a decrease in the rate of cleavage C.

In general, protections from proteolysis are difficult to interpret, as they can result from occlusion of the protease-sensitive site by the ligand or from a conformational change. If the protection by ADP were due to occlusion of the cleavage site, then AMP−PNP would also be expected to give the protection. However, AMP−PNP does not protect cleavage site C relative to what is observed for the free enzyme (Figure 6a, $E^{33/32}$ in No Ligand vs AMP−PNP lanes; see also Figure 7b). The data therefore suggest that the ADP-induced protections from proteolysis result from a conformational change in eIF4A.

The inhibition of cleavage C upon ADP binding also suggests that the proteolytic fragments remain associated with one another after cleavage at sites B/B′ (Figure 1a). The B/B′ cleavage sites occur on the C-terminal side of the Walker A motif (GxGKT; Figure 1b), which is expected to be an integral part of the enzyme's nucleotide binding site (*22*). If this fragment were to dissociate from the E^{23} fragment, a functional nucleotide binding site would no longer exist so that ADP could not affect the protease sensitivity of E^{23}.

Structural Distinctions among the Enzyme·Ligand Complexes. In the above sections, the conformation of free eIF4A was compared with the conformations of the binary complexes E·ssRNA and E·ADP. The data described above provide no indication of a conformational change upon binding of AMP−PNP to the free enzyme (Figures 4a and 6a). However, binding of both ssRNA and ADP to the free enzyme induces conformational changes, and the resulting binary complexes, E·ssRNA and E·ADP, are conformationally distinct from one another. In the following sections, data are presented that suggest that free eIF4A and its binary complexes are conformationally distinct from the ternary complexes, E·AMP−PNP·ssRNA and E·ADP·ssRNA and, further, that the ternary complexes are conformationally distinct from each other.

Each Enzyme·Nucleotide Complex Is Conformationally Distinct from the Corresponding Enzyme·Nucleotide·ssRNA Complex. For each nucleotide, the proteolysis data suggest that the enzyme·nucleotide complex is conformationally distinct from the enzyme·nucleotide·ssRNA complex (Figure 3). Proteolysis at sites A and C is increased upon binding of ssRNA to E·AMP−PNP. For the A cleavage, this can be seen by comparing the AMP−PNP lanes in Figure 4a with the RNA + AMP−PNP lanes of Figure 5 (note that the trypsin concentration is 10-fold higher in Figure 4a than in Figure 5). For the C cleavage, the difference can be seen by comparing the AMP−PNP and RNA + AMP−PNP lanes of Figure 6a.

The data also suggest that the E·ADP and E·ADP·ssRNA complexes are conformationally distinct from each other (Figure 3). Cleavage at site A (e.g., Figure 4a, ADP lanes vs Figure 5 RNA + ADP lanes; note the difference in trypsin concentration) and cleavage at site B/B′ (e.g., Figure 6a, ADP vs RNA + ADP lanes) are 5−10-fold faster

in the E·ADP·ssRNA complex than in the E·ADP complex.

Binding of Nucleotides to the E·ssRNA Complex Induces Conformational Changes, and the Resultant Ternary Complexes Are Conformationally Distinct. The proteolysis experiments also suggest that binding of ADP and AMP−PNP to the E·ssRNA complex each causes conformational changes in this species. In addition to being distinct from the E·ssRNA and E·nucleotide binary complexes, the ternary complexes, E·AMP−PNP·ssRNA and E·ADP·ssRNA, are also distinct from one another. The data leading to these conclusions are described below and summarized in Figure 3 for clarity.

Cleavage A, which is shown in Figure 5, is approximately 2-fold slower for the E·ADP·ssRNA complex ($t_{1/2} \approx 0.4$ min) than for the E·ssRNA or E·AMP−PNP·ssRNA complexes ($t_{1/2} \approx 0.2$ min for both complexes; see also Table 1). While this difference in the rate of cleavage A is small, it is reproducible and easily detectable. The rate of cleavage B/B′ is also decreased ∼2-fold upon binding of ADP to the E·ssRNA complex (Figures 4a and 6a and data not shown). Most strikingly, the $E^{23/22}$ fragment (cleavage C), which is produced from the E·ssRNA and E·AMP−PNP·ssRNA complexes, is not formed from the E·ADP·ssRNA complex (Figure 6a, RNA + ADP lanes; see also "*Binding of ADP·Mg^{2+} to the free enzyme produces a conformational change*" above). This difference provides additional evidence that the E·ADP·ssRNA complex is conformationally distinct from the E·ssRNA and E·AMP−PNP·ssRNA complexes.

In contrast to the effects observed upon binding of ADP to the E·ssRNA complex, there is no difference in the rate of cleavage at site A between the E·AMP−PNP·ssRNA and E·ssRNA complexes (Figure 5, RNA vs RNA + AMP−PNP lanes). Binding of AMP−PNP to E·ssRNA does, however, decrease the rate of cleavage at site B/B′, and the decrease is 2−3-fold larger than the decrease caused by binding of ADP (Figure 6a, RNA vs RNA + AMP−PNP lanes; also compare to RNA + ADP). The possibility that this protection is due to the occlusion of the B/B′ cleavage site upon AMP−PNP binding cannot be ruled out, although AMP−PNP does not protect this site when it binds to the free enzyme (Figure 6a, No Ligand vs AMP−PNP lanes). Regardless, the ∼10-fold higher efficiency of UV cross-linking of RNA to the E·AMP−PNP·ssRNA complex than to the E·ssRNA and E·ssRNA·ADP complexes (*14*) strongly suggests that binding of AMP−PNP to the E·ssRNA complex induces a conformational change and that this conformational change is distinct from the one induced by ADP binding.

The patterns of chymotrypsin proteolysis also suggest that the E·AMP−PNP·ssRNA and E·ADP·ssRNA complexes are different conformationally. The 46.5 kDa fragment accumulates to a greater extent from E·AMP−PNP·ssRNA than from E·ADP·ssRNA (Figure 4b, compare RNA + AMP−PNP and RNA + ADP lanes). In contrast, more of the 33 kDa fragment is generated from E·ADP·ssRNA than from E·AMP−PNP·ssRNA (Figure 4b, compare RNA + AMP−PNP and RNA + ADP lanes). This is analogous to the effects with trypsin (see above and Table 1) and further suggests that the E·AMP−PNP·ssRNA and E·ADP·ssRNA species are conformationally distinct. Furthermore, full-length eIF4A is cleaved by chymotrypsin ∼5-fold faster in the E·ssRNA complex than in the E·AMP−PNP·ssRNA or E·ADP·ssRNA complexes (Figure 4b, RNA 10-min lane vs RNA + AMP−PNP and RNA + ADP 60-min lanes). This is consistent with the latter species being conformationally different than the E·ssRNA complex.

The above proteolysis data with both trypsin and chymotrypsin suggest that the E·ssRNA, E·AMP−PNP·ssRNA, and E·ADP·ssRNA complexes are conformationally distinct from one another (Figure 3). The differences in the efficiency of UV-induced RNA cross-linking among these states, presented in the preceding paper in this issue and summarized in Figure 3, provide further evidence for this conclusion (*14*).

ATP Binding and Conformational Changes

As coupling is observed between the binding of ATP and ssRNA but not AMP−PNP and ssRNA, the following question arises: How are the conformational changes produced by AMP−PNP related to what takes place upon ATP binding? The coupling between the binding of ATP and ssRNA suggests that ATP binding also causes a conformational change in eIF4A. ATP produces similar changes in protease sensitivity to AMP−PNP upon binding to E·ssRNA, but the effects are smaller (data not shown), as expected because it is hydrolyzed to produce ADP during the course of the experiment. This suggests that ATP and AMP−PNP stabilizes similar enzyme conformations. Both ATP and AMP−PNP induce increases in the efficiency of the enzyme's UV cross-linking to RNA, further suggesting that, in the presence of ssRNA, ATP and AMP−PNP binding stabilize related enzyme conformations. As described in the previous section, these conformations appear to be distinct from those stabilized by ssRNA binding alone and by ADP binding in the presence or absence of ssRNA.

Buffer Conditions Affect the Conformation of eIF4A: Implications for Coupled Binding between Nucleotides and ssRNA

As shown in the preceding paper in this issue, there is coupling between the binding of nucleotides and ssRNA under one set of buffer conditions but not under another set of conditions (B and A conditions; see the Experimental Procedures section). This led to a proposal that there are conformational changes that occur upon ligand binding under buffer conditions B that do not occur under buffer conditions A (*14*). Consistent with this proposal, some of the conformational changes detected in the proteolysis experiments with buffer conditions B are not detected with buffer conditions A.

Under buffer conditions B, the rates of cleavages A, B/B′, and C are each different among free enzyme, E·ssRNA and E·ADP·ssRNA, but under buffer conditions A, only the production of the 23 kDa fragment is significantly different between the E·ADP·ssRNA complex and the free enzyme or E·ssRNA complex (Figure 6a vs Figure 8). These data suggest that there are fewer conformational states accessible to the enzyme under buffer conditions A than under buffer conditions B. Most strikingly, under buffer conditions A, the large increase in protease sensitivity upon ssRNA binding does not occur (Figure 8). These results support the proposal that the lack of energetic coupling between nucleotide and

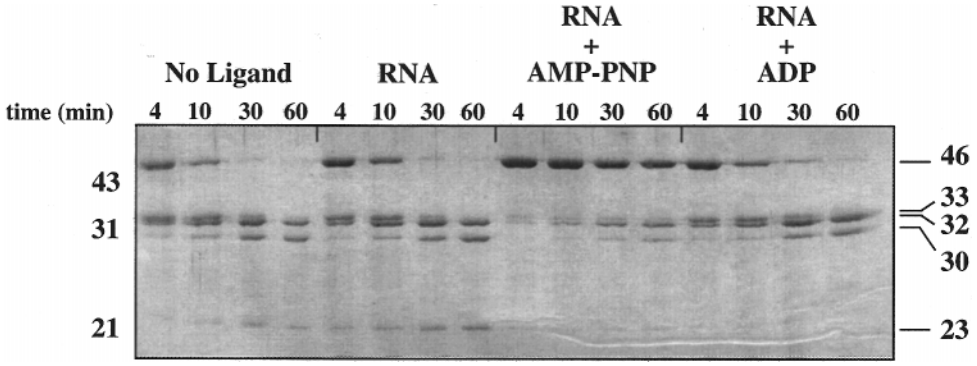

FIGURE 8: Different enzyme conformations are stabilized under buffer conditions A than under buffer conditions B. Same as in Figure 6a (400 nM trypsin) except that buffer conditions A were used instead of buffer conditions B, 300 μM poly(U) was used, and samples were analyzed on a 15% SDS poly(acrylamide) gel instead of a 10% gel. The buffer conditions are defined in the Experimental Procedures section. Molecular weight markers (kDa) are shown to the left and the approximate size of each fragment to the right.

ssRNA binding under buffer conditions A is the result of conformational differences in the various enzyme complexes under the two buffer conditions (*14*).

A ~30 kDa fragment accumulates to a much greater extent with buffer conditions A than it does with conditions B (Figures 6 and 8), further suggesting that the conformations of the enzyme can change with changing salt and pH conditions. It will be interesting to determine if buffer effects mimic the effects of the interaction of other translation initiation factors with eIF4A (*14*).

DISCUSSION

The data presented in this and the preceding paper in this issue suggest that eIF4A undergoes a cycle of ligand-dependent conformational changes as it binds its substrates, hydrolyzes ATP, and releases products. These data are summarized in Figure 3. The patterns of proteolysis and protease sensitivities of the free enzyme, E•ssRNA, E•ADP, E•AMP−PNP•ssRNA, and E•ADP•ssRNA complexes are different from one another, suggesting that the binding of these ligands to the enzyme stabilizes different protein conformations. The changes in the efficiency of UV cross-linking of RNA to the E•ssRNA, E•AMP−PNP•ssRNA, E•ATP•ssRNA, and E•ADP•ssRNA complexes also suggest that these complexes are conformationally different from one another (*14*). As discussed in the following section, the data also suggest that the nucleotide-dependent conformational changes, like the changes in RNA affinity described in the preceding paper in this issue (*14*), are mediated by the presence or absence of the γ-phosphate.

Transducing the Energy from ATP Hydrolysis into Work: The Walker Motif. Enzymes that convert the chemical energy from NTP hydrolysis into work do so by changing conformation and ligand affinity depending on the nucleotide bound in their active sites. Ion pumps (*23*), molecular motors such as myosin (*24*) and kinesin (*25*), and G-proteins such as EF-Tu (*26*) and EF-G (*27*) operate on this principle. DNA helicases appear to unwind duplex DNA using similar principles, and there is evidence that a number of DNA helicases undergo ligand-dependent conformational changes (*28*−*32*).

Structural studies have demonstrated that in NTPases containing the conserved Walker motifs (*22*), conformational changes are mediated by contacts between the protein and the γ-phosphate of the NTP and the Mg^{2+} chelated to the β- and γ-phosphates of the NTP (for reviews, see refs 33 and 34); (Figure 9). A key residue in this conformational change is the invariant aspartate of the Walker B motif (the first Asp in the DEAD motif of the DEAD box proteins), which appears to bind the Mg^{2+} via a water molecule (Figure 9). Upon NTP hydrolysis and inorganic phosphate release, the position of this Mg^{2+} moves, inducing conformational changes in the enzyme. Direct contacts to the γ-phosphate are also disrupted upon NTP hydrolysis. For example, the lysine of the GKT sequence of the Walker A motif makes a direct contact with the β- and γ-phosphates of the bound NTP. eIF4A has both the Walker A and B motifs (Figure 1b), and thus, it is likely that the ATP- and ADP-induced conformational changes are mediated by similar mechanisms in this enzyme.

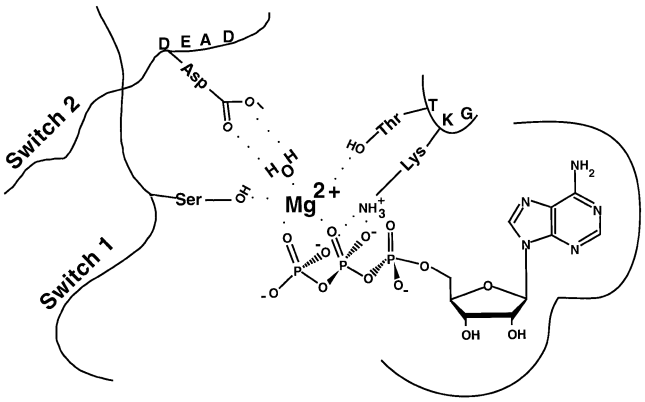

FIGURE 9: Schematic diagram of the active site of a Walker NTPase. The positions of the Walker A motif (GKT) and DEAD sequence (Walker B) of the DEAD box proteins are also shown. Switch 1 and switch 2 are regions of the Walker NTPases involved in transducing conformational changes dependent on the presence or absence of the γ-phosphate on the bound NTP•Mg^{2+} (*33*). As depicted, the residue in switch 1 that contacts the Mg^{2+} is a Ser or Thr in known cases (*34*).

The binding, cross-linking, and proteolysis data presented in this and the preceding paper in this issue (*14*) provide evidence that ATP•Mg^{2+} and ADP•Mg^{2+} stabilize different states of the enzyme and modulate the enzyme's affinity for ssRNA. These differences among enzyme complexes indicate that the presence or absence of a γ-phosphate on the bound adenosine nucleotide modulates the conformation of the E•ssRNA complex (Figure 3). This suggests that the γ-phosphate is used as a switch to change the conformation of eIF4A such that ATP binding and hydrolysis produce a

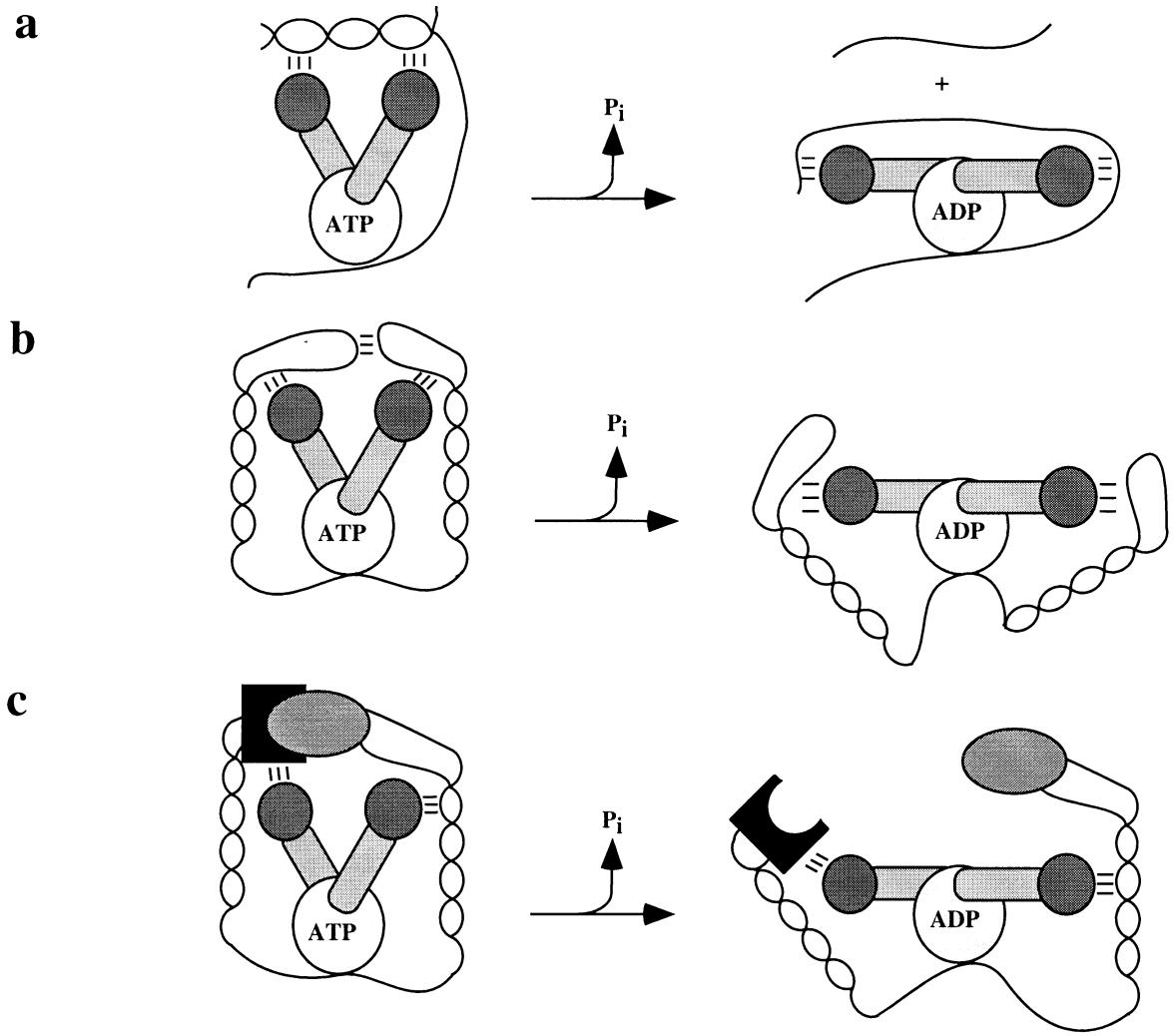

FIGURE 10: Highly schematic model showing the proposed function of the DEAD box core domain (unshaded circles) as a motor that uses the energy from ATP hydrolysis to produce conformational changes in or movements of attached protein domains or associated proteins (dark gray circles). Sections a−c show different forms of work that could be generated in this way, depending on what domains are attached or proteins associated with the core DEAD box motor: (a) unwinding of structured RNA; (b) rearrangement of RNA tertiary structures; (c) disruption or alteration of protein−protein (or protein-RNA) interactions within an RNA•protein complex.

cycle of conformational changes in the enzyme. When ATP binds to the E•ssRNA complex it stabilizes one conformation of the enzyme. Upon hydrolysis of ATP to ADP, a conformational change takes place, followed by another one when ADP is released. As described in the next section, such a cycle of conformational changes could, in principle, be used to perform work on RNA and/or protein substrates.

It has been proposed, based on crystallographic studies, that a series of β-strands in the core of RecA and the Rep DNA helicase are involved in transducing conformational changes between the ATPase and DNA binding sites of these enzymes (*21, 35*). Rep has sequence similarities to eIF4A (*19, 20*), and the regions of Rep expected to correspond to the positions of cleavages B/B′ and C are loops that run from these core regions to regions of the core that contact the ssDNA ((ref 21) and M. Peck, J.R.L. and D. H., Unpublished Results). Thus, the cleavage sites are in regions that might be expected to undergo motion in the course of nucleotide and nucleic acid binding to eIF4A.

General Proposal for the Function of the Core DEAD Box Domain. While neither the nucleotide-dependent modulation of RNA affinity nor the conformational changes described in this and the preceding paper in this issue (*14*) explain the function or mechanism of eIF4A or other DEAD box proteins, the data represent a step toward understanding the molecular basis for the action of these enzymes. The data also suggest a general model for the operation of eIF4A and the eIF4A-like domains of the DEAD box proteins (Figure 10). The fact that eIF4A, which is essentially the core domain of all the DEAD box proteins (*5*), undergoes a cycle of ligand-dependent conformational changes raises the possibility that all of these proteins undergo similar cycles. Thus, the role of the eIF4A-like core domain may be to bind to RNA and to transduce the energy from ATP hydrolysis into protein motion—i.e., act as a motor. This motion could then be used to perform different tasks depending on what other protein domains are attached to the core eIF4A-like domain or what other proteins are bound to it (Figure 10). The motions of the eIF4A-like domain could produce motions of or rearrangements in attached protein domains or associated proteins. These motions would, in turn, be used to rearrange the RNA, protein, or RNA−protein complex that is the substrate of the particular DEAD box protein (Figure 10). The substrate or target of a particular DEAD box protein would be determined by what "adapter" domains or

associated proteins are attached or bound to the core DEAD box motor (Figure 10).

The RNA binding site on the core domain could be an integral component of the mechanism of substrate rearrangement, could be used to recognize specific RNA substrates, or could serve as the attachment point to allow rearrangement of nearby RNA and/or protein elements. Once a DEAD box protein has bound its RNA substrate, hydrolyzed ATP, and transduced the energy from this hydrolysis into work to perform its particular molecular function (e.g., dsRNA unwinding), it may then be beneficial for the enzyme to dissociate from its substrate so that another step in the process in which the enzyme operates can occur (e.g., binding of the 40S ribosomal subunit in translation initiation). The 40-fold weakening of ssRNA affinity between the E·ATP and E·ADP complexes would make mechanistic sense in this light. Alternatively, the affinity switches could be used directly, in conjunction with the conformational changes, to rearrange RNA structures or RNA−protein complexes.

What Do the DEAD Box Proteins Do? The model proposed above for the DEAD box proteins is analogous to the apparent mechanism of action of the G-proteins and the motor proteins myosin and kinesin: A common structurally conserved core element transduces the energy of NTP hydrolysis into motion and thus, in conjunction with the remainder of the protein, into work (*33, 34*). The functions of these proteins are different (e.g., intracellular signaling via protein−protein interactions, maintenance of fidelity in macromolecular interactions, motion in different directions along filaments), but the underlying mechanism for their operation may be the same.

Similarly, the DEAD box proteins all share a similar core domain and thus may have a common underlying mechanism of action. They need not, however, perform the exact same function. Some may be "RNA helicases" (Figure 10a), although it is unlikely that a protein that untangles RNA structures would perform the same function as a canonical helicase. This is because the substrates that RNA helicases would encounter are smaller, less regular structures than those that canonical helicases encounter. The DEAD box proteins involved in the replication of viral genomes (*19, 36, 37*), which might have to contend with longer stretches of RNA duplexes, are likely to be exceptions to this suggestion, however. Other DEAD box proteins could perform functions distinct from RNA unwinding. These possible functions include (1) mediating larger scale RNA structural rearrangements (Figure 10b) (*38*−*40*); (2) altering protein−RNA or protein−protein interactions, analogous to the disruption of protein-DNA contacts in the nucleosome by the Swi/Snf complex (Figure 10c; the ATPase of the Swi/Snf complex, Swi2/Snf2, is related to the DEAD box family (*41*, *42*−*45*)); and (3) functioning, as the G-protein EF-Tu does, as a guarantor of fidelity in RNA−RNA interactions and rearrangements (*46*). There is no reason to assume a priori that all members of a sequence family of proteins perform the same function.

eIF4A may transduce the ATP hydrolysis-driven structural rearrangements into work through an associated initiation factor, for example, eIF4B. The resultant work could be in the form of unwinding of RNA structures (Figure 10a). eIF4A, in conjunction with eIF4B, can unwind duplex RNAs in vitro, but it is not yet clear if this unwinding activity is efficient enough to represent a plausible in vivo function for the enzyme. Furthermore, it is not yet possible to rule out other functions for eIF4A, such as the disruption of protein−protein or protein−RNA contacts or larger scale RNA structural rearrangements. More work is required to elucidate the molecular functions of eIF4A and the other DEAD box proteins. The kinetic, thermodynamic, and conformational frameworks presented in this and the preceding paper in this issue should serve as starting points for future mechanistic studies of eIF4A. The information obtained with eIF4A may also facilitate unraveling the mechanisms and functions of other members of the DEAD box family of RNA-dependent ATPases.

ACKNOWLEDGMENT

We are grateful to Nathalie Methot for advice and discussions and to Nahum Sonenberg for supplying plasmids and for advice. We thank Kathy Suri for technical assistance; Alan Sachs and members of our laboratory for advice, discussions, and comments on the manuscript; Myron Crawford and Kathy Stone for advice on peptide sequencing; and Gabriel Waksman for providing the coordinates for the Rep helicase·DNA complex. N-Terminal sequence analysis was performed at the W. M. Keck Foundation Biotechnology Resource Laboratory at Yale University.

REFERENCES

1. Grifo, J. A., Abramson, R. D., Satler, C. A., and Merrick, W. C. (1984) *J. Biol. Chem. 259*, 8648−8654.
2. Pause, A., and Sonenberg, N. (1992) *EMBO J. 11*, 2643−2654.
3. Benne, R., and Hershey, J. W. B. (1979) *J. Biol. Chem. 253*, 3078−3087.
4. Anthony, D. D., and Merrick, W. C. (1992) *J. Biol. Chem. 267*, 1554−1562.
5. Schmid, S. R., and Linder, P. (1992) *Mol. Microbiol. 6*, 283−292.
6. Rozen, F., Edery, I., Meerovitch, K., Dever, T. E., Merrick, W. C., and Sonenberg, N. (1990) *Mol. Cell. Biol. 10*, 1134−1144.
7. Ray, B. K., Lawson, T. G., Kramer, J. C., Cladaras, M. H., Grifo, J. A., Abramson, R. D., Merrick, W. C., and Thach, R. E. (1985) *J. Biol. Chem. 260*, 7651−7658.
8. Lawson, T. G., Lee, K. A., Maimone, M. M., Abramson, R. D., Dever, T. E., Merrick, W. C., and Thach, R. E. (1989) *Biochemistry 28*, 4729−4734.
9. Pause, A., Methot, N., and Sonenberg, N. (1993) *Mol. Cell. Biol. 13*, 6789−6798.
10. Hirling, H., Scheffner, M., Restle, T., and Stahl, H. (1989) *Nature 339*, 562−564.
11. Lain, S., Riechmann, J. L., and Garcia, J. A. (1990) *Nucleic Acids Res. 18*, 7003−7006.
12. Shuman, S. (1992) *Proc. Natl. Acad. Sci. U.S.A. 89*, 10935−10939.
13. Flores-Rozas, H., and Hurwitz, J. (1993) *J. Biol. Chem. 268*, 21372−21383.
14. Lorsch, J. R., and Herschlag, D. (1998) *Biochemistry 37*, previous paper in this issue.
15. Abramson, R. D., Dever, T. E., Lawson, T. G., Ray, B. K., Thach, R. E., and Merrick, W. C. (1987) *J. Biol. Chem. 262*, 3826−3832.
16. Goss, D. J., Woodley, C. L., and Wahba, A. J. (1987) *Biochemistry 26*, 1551−1556.
17. Sambrook, J., Fitsch, E. F., and Maniatis, T. (1989) *Molecular Cloning. A Laboratory Manual*, Cold Spring Harbor Laboratory Press: Cold Spring Harbor, NY.
18. Erlanger, B. F., Kokowsky, N., and Cohen, W. (1961) *Arch. Biochem. Biophys. 95*, 271−278.

19. Gorbalenya, A. E., Koonin, E. V., Donchenko, A. P., and Blinov, V. M. (1988) *FEBS Lett. 235*, 16−24.
20. Seki, M., Miyazawa, H., Tada, S., Yanagisawa, J., Yamaoka, T., Hoshino, S., Ozawa, K., Eki, T., Nogami, M., Okumura, K.,Taguchi, H., Hanaoka, F., and Enomoto, T. (1994) *Nucleic Acids Res. 22*, 4566−4573.
21. Korolev, S., Hsieh, J., Gauss, G. H., Lohman, T. M., and Waksman, G. (1997) *Cell 90*, 635−647.
22. Walker, J. E., Saraste, M., Runswick, M. J., and Gay, N. J. (1982) *EMBO J. 1*, 945- 951.
23. Jencks, W. P. (1989) *J. Biol. Chem. 264*, 18855−18858.
24. Spudich, J. A. (1994) *Nature 372*, 515−518.
25. Gilbert, S. P., Webb, M. R., Brune, M., and Johnson, K. A. (1995) *Nature 373*, 671- 676.
26. Abel, K., and Jurnak, F. (1996) *Structure 4*, 229−238.
27. Rodnina, M. V., Savelsbergh, A., Katunin, V. I., and Wintermeyer, W. (1997) *Nature 385*, 37−41.
28. Nakayama, N., Arai, N., and Arai, K. (1984) *J. Biol. Chem. 259*, 88−96.
29. Chao, K., and Lohman, T. M. (1990) *J. Biol. Chem. 265*, 1067−1076.
30. Yong, Y., and Romano, L. J. (1995) *J. Biol. Chem. 270*, 24509−24517.
31. Jezewska, M. J., and Bujalowski, W. (1996) *J. Biol. Chem. 271*, 4261−4265.
32. Korolev, S., Hsieh, J., Gauss, G. H., Lohman, T. M., and Waksman, G. (1997) *Cell 90*, 635−647.
33. Smith, C. A., and Rayment, I. (1996) *Biophys. J. 70*, 1590−1602.
34. Vale, R. D. (1996) *J. Cell Biol. 135*, 291−302.
35. Story, R. M., and Steitz, T. A. (1992) *Nature 355*, 374−376.
36. Gorbalenya, A. E., Koonin, E. V., and Wolf, Y. I. (1990) *FEBS Lett. 262*, 145−148.
37. Gorbalenya, A. E., and Koonin, E. V. (1989) *Nucleic Acids Res. 17*, 8414−8440.
38. Guthrie, C. (1994) *Harvey Lect. 90*, 59−80.
39. O'Day, C. L., Dalbadie-McFarland, G., and Abelson, J. (1996) *J. Biol. Chem. 271*, 33261- 33267.
40. Kim, S.-H., and Lin, R.-J. (1996) *Mol. Cell. Biol. 16*, 6810−6819.
41. Bork, P., and Koonin, E. V. (1993) *Nucleic Acids Res. 21*, 751−752.
42. Winston, F., and Carlson, M. (1992) *Trends Genet. 8*, 387−391.
43. Cote, J., Quinn, J., Workman, J. L., and Peterson, C. L. (1994) *Science 265*, 53−60.
44. Laurent, B. C., Treich, I., and Carlson, M. (1993) *Genes Dev. 7*(4), 583−591.
45. Auble, D. T., Hansen, K. E., Mueller, C. G., Lane, W. S., Thorner, J., and Hahn, S. (1994) *Genes Dev. 8*, 1920−1934.
46. Burgess, S. M., and Guthrie, C. (1993) *Trends Biochem. Sci. 18*, 381−384.

BI9724319